From intermediate valence to magnetic behavior without long-range order by hydrogenation of the ternary gallide CeNiGa.

Bernard Chevalier, Jorge Sánchez Marcos, Jesus Rodríguez Fernández, Mathieu Pasturel, François Weill

From intermediate valence to a magnetic behavior without long-range order by hydrogenation of the ternary gallide CeNiGa.

B. Chevalier, J. Sanchez Marcos, J. Rodriguez Fernandez, M. Pasturel and F. Weill

Abstract

We have studied both the crystal chemistry and magnetic, transport and thermal properties of the hydride $CeNiGaH_{1.1(1)}$. This compound crystallizes in the hexagonal AlB_2-type structure with a random distribution of nickel and gallium atoms on the B-site, which has an important influence upon the macroscopic properties. Its thermoelectric power versus temperature indicates that cerium is in trivalent state. The electrical resistivity displays two minima, which could be expected for the Kondo type interactions in the presence of crystal field effects. Specific heat measurements up to 300 K allow us to determine the CEF splitting energies Δ_1 = 100 K and Δ_2 = 159 K. A broad maximum is observed around 4 K in the specific heat in the low temperature region. This maximum and its evolution with the applied magnetic field, are discussed in the framework of the existing theories, which point towards the existence of short range magnetic correlations and spin glass like freezing below 1.8 K. This study reveals : (i) that the hydrogenation of the intermediate valence gallide CeNiGa induces a valence transition for cerium which is purely trivalent in the hydride and (ii) the absence above 1.8 K of long-range magnetic ordering resulting from structural disorder around Ce-atoms.

I. Introduction

The use of extreme conditions is an important way to induce new physical properties of materials. Over the last few years, in addition to the low temperatures and high magnetic fields, the development of more performance pressure cells has made it possible to extend the use of high pressure and consequently to discover new phenomena such as the coexistence of magnetism and superconductivity,[1] the appearance of quantum phase transition [2] or the induction of magnetic order in a spin liquid compound.[3] From this point of view, hydrogen insertion into the lattice can give rise an important increase in the volume and therefore act as a negative chemical pressure which induces new properties in the materials.

In particular the hydrogenation of intermetallic compounds based on cerium is an interesting route in order to modify the competition between the Kondo effect and the magnetic RKKY interaction which governs their physical properties. This competition was explained using the magnetic phase diagram proposed by Doniach.[4] The Kondo effect and RKKY interaction depend differently on the coupling constant J_{cf} between 4f(Ce) and conduction electrons which is affected both by the 4f(Ce)-conduction electrons mixing and the location of the 4f(Ce) level E_{4f} relative to E_F Fermi level: (i) if E_{4f} is well separated to E_F, J_{cf} is small and the 4f(Ce) electrons show a normal localized state with magnetic moments; (ii) when E_{4f} approaches E_F, J_{cf} increases and the compound begins to exhibit Kondo-like behavior (the magnetic ordering temperature and the magnetic ordered moment are reduced); (iii) when J_{cf}, is increased even more, the compound goes into the non-magnetic valence fluctuation regime. Considering this diagram, the hydrogenation can produce an interesting transition from a valence fluctuation ground state to a magnetically ordered or even "heavy fermion" ground state. Indeed, the hydrogen insertion into the lattice generally induces an increase in the unit cell volume leading to a reduction in the coupling constant J_{cf}.

Recently, we have shown that the hydrogenation of the two CeNiGa crystallographic forms (LTF and HTF respectively for Low and High Temperature Form) classified as

intermediate valence compounds leads to the formation of the hydride $CeNiGaH_{1.1(1)}$.[5] The synthesis of this hydride is accompanied by a large increase of the molar unit cell volume V_m; respectively +19.3 % and +15.6 % after hydrogenation of LTF and HTF. If we use a weighted average of the compressibility of the constituents elements in the solid state, as was done by de Visser et al. [6] in the absence of data on the real compressibility, the increase in V_m from CeNiGa LTF corresponds to a negative pressure of ≅ -4 GPa. Our preliminary characterization of $CeNiGaH_{1.1(1)}$ by magnetization measurements suggests that the cerium is trivalent. In other words, the hydrogenation of CeNiGa induces a valence transition for cerium from the intermediate valence state (CeNiGa LTF and HTF) to a purely trivalent state ($CeNiGaH_{1.1(1)}$). Moreover, this hydride presents above 1.8 K no sign of any occurrence of a long-range magnetic ordering, suggesting perhaps a "heavy fermions" behavior. In order to solve this question, we have performed electrical resistivity, thermoelectric power, magnetoresistivity and specific heat measurements on $CeNiGaH_{1.1(1)}$. It was found that below 4 K short magnetic correlations exist in this hydride. This behavior results from the statistical distribution of Ni and Ga atoms at the same crystallographic site and also the partial occupancy of the site devoted to H atoms. These structural properties induce some randomness in Ce-Ce exchange interactions. The results are discussed in relation to those reported on Ce_2NiGe_3 [7] and Ce_2CuGe_3,[8] which crystallize as $CeNiGaH_{1.1(1)}$, in a derivative structure of the hexagonal AlB_2-type.

II. Experimental details

The polycrystalline samples of the ternary gallide CeNiGa and its hydride were synthesized and characterized by X-ray powder diffraction as previously described in ref. 5.

For electron microscopy experiments (JEOL 2000FX), parts of the hydride $CeNiGaH_{1.1(1)}$ were crushed in ethanol in an agate mortar and the small fragments were placed on a copper grid covered with an amorphous perforated carbon film.

For transport measurements, the hydride was compacted at room temperature (compactness ≅ 80%) in order to form a polycrystalline pellet (diameter = 6 mm and thickness = 3 mm) and then heated for two days at 523 K under pressure (5 MPa) of hydrogen. Thermoelectric power measurements were performed on this pellet using a dynamic method. Details of the cell used and measurement methods have been described previously. [9] For electrical resistivity, a bar of 1.5 x 1.5 x 5 mm^3 was cut from the pellet. The measurement was carried out above 1.8 K using the standard dc four probe method with silver paint contacts and an intensity current of 10 mA. Magnetoresistivity research was performed down to 2 K for applied magnetic fields 0 T≤ $\mu_0 H$ ≤ 9 T on the same bar using PPMS Quantum Design system. Finally, magnetization measurements were performed on a part of the pellet using a Superconducting Quantum Interference Device (SQUID) magnetometer in the temperature range 1.8-300 K and applied fields up to 5 T.

Heat capacity measurements on hydride $CeNiGaH_{1.1(1)}$ were performed by a relaxation method with a Quantum Design PPMS system and using a two tau model analysis. Data were taken in the 2-300 K temperature range under applied magnetic fields of 0, 3, 6 and 9 T. For these latter measurements, the sample was a plate of 0.3 mm thickness and a 8.13 mg weight obtained from the same pellet used for the transport and magnetization measurements.

III. Results and discussion

Our investigation on the structural properties of the hydride $CeNiGaH_{1.1(1)}$ using X-ray powder diffraction indicates that it crystallizes in the hexagonal AlB_2-type structure (space group P6/mmm) with a = 4.239(4) Å and c = 4.258(5) Å as unit cell parameters. [5] In this structure, the Ni- and Ga-atoms are randomly distributed on the same crystallographic site; this distribution can be expected to cause some anomalous physical properties. For instance,

the ternary germanides Ce_2NiGe_3 [7] and Ce_2CuGe_3, [8] which adopt the hexagonal AlB_2-type with a random distribution of Ni- or Cu- and Ge-atoms, exhibit at low temperature a nonmagnetic atom disorder spin glass behavior.

In order to confirm this crystal structure, we have examined some small crystals of this hydride by transmission electron microscopy. Typical electron diffraction patterns projected along the [0 –1 0] zone axis of the subcells of $CeNiGaH_{1.1(1)}$ and $CeNiSnH_{1.8(2)}$ are shown in Fig. 1. It can clearly be ruled out that the lattice parameter c = 8.543(2) Å of $CeNiSnH_{1.8(2)}$ is twice that corresponding to $CeNiGaH_{1.1(1)}$. The former hydride adopts the hexagonal ZrBeSi-type, which is a variant of the AlB_2-type with an ordering of the Ni- and Sn-atoms.[10] This atomic ordering induces the relation $c_{ZrBeSi} = 2\ c_{AlB2}$. The present study confirms the structural properties of the hydride $CeNiGaH_{1.1(1)}$. We note also that $CeNiGaH_{1.1(1)}$ shows the same structural properties as the other hydride $CeNiAlH_{1.93(5)}$,[11] but contains a much smaller hydrogen concentration. The partial occupancy of the crystallographic site devoted to the H-atoms also induces structural disorder around the Ce-atoms.

A. Magnetization

Above 100 K, the magnetic susceptibility χ_m of $CeNiGaH_{1.1(1)}$ follows a Curie-Weiss law with θ_p = -100 K as the paramagnetic Curie temperature and μ_{eff} = 2.52 μ_B/Ce as the effective moment.[5] This last value is very close to that calculated for a free Ce^{3+} ion (2.54 μ_B). Moreover, the large negative value of θ_p suggests that the Kondo effect plays an important role on the physical properties of this hydride.

At low temperatures, an interesting result is derived from comparing the temperature dependence of the magnetic susceptibility of $CeNiGaH_{1.1(1)}$ measured in zero-field-cooled (ZFC) and field-cooled (FC) modes (Fig. 2). A small irreversibility effect appears below T_{IR} = 4 K, but the absence of peak above 1.8 K on the curve χ_{ZFC} = f(T) does not allow us to define a freezing temperature. Irreversibility is a typical feature expected for spin glasses.[12] In the same way, another characteristic of all the materials showing spin glass behavior is the remanence that can be observed when the applied magnetic field is changed below the irreversibility temperature T_{IR}. The inset of Fig. 3 shows the hysteresis of the magnetization of the hydride measured at 2 K; the remanence is about 0.001 μ_B per Ce-atom. The coercive field takes a small value close to 50 Oe. Finally, we note that the field dependence of magnetization at 2 K exhibits a curvature but is still not saturated at $\mu_0 H$ = 5 T (Fig. 3). All these results rule out the presence of long-range magnetic ordering for $CeNiGaH_{1.1(1)}$. Furthermore, although it exhibits some typical features observed in spin glasses, the susceptibility shape does not resemble those commonly found in these materials; in addition, the ac susceptibility shows no peak at low temperature, as is always observed in spin glasses. These results suggest that the freezing temperature could be smaller than 1.8 K. Therefore, the irreversibility effect observed for this hydride might be interpreted in terms of short-range magnetic interactions dictated by crystallographic disorder.

B. Electrical resistivity and thermoelectric power

The temperature dependence of the electrical resistivity of $CeNiGaH_{1.1(1)}$ is depicted in Fig. 4. Before explaining its behavior and in order to understand it, we should make reference to the electrical resistivity measurements of CeNiGa LTF and HTF, which can be summarized as follows:[5] (i) the curve ρ = f(T) relative to CeNiGa LTF exhibits a quadratic temperature dependence between 4.2 and 70-75 K and then increases linearly with the temperature, which characterizes a nonmagnetic metal where the 4f(Ce) electrons are strongly delocalised; the Kondo temperature T_K of CeNiGa LTF was estimated to be 1000 K; (ii) in contrast, the magnetic part of the electrical resistivity of CeNiGa HTF shows a broad maximum centred

around 75 K as in the intermediate valence cerium compounds; in this case $T_K \approx 95(5)$ K was determined from the magnetic susceptibility measurements.

The electrical resistivity ρ of $CeNiGaH_{1.1(1)}$, exhibits a different behavior (Fig. 4). First, there is a large value of the residual resistivity RR = ρ(1.8 K) = 6940 μΩ.cm and a small residual resistivity ratio RRR = ρ(300 K)/ρ(1.8 K) = 1.05. Two hypotheses can be proposed in order to explain these values that are unusual for a normal metal; they can be attributed to: (i) the presence of many porosities and micro cracks resulting from the low temperature (523 K) used during the annealing treatment performed on the sample or (ii) the scattering due to the structural disorder as is usually observed in metallic spin glasses. It is interesting to note that the similar measurements performed on the hydrides $CeNiSnH_{1.0}$ and $CeNiSnH_{1.8}$ where Ni and Sn atoms are structurally ordered, give a higher RRR factor; 2.00 and 1.87 for $CeNiSnH_{1.0}$ and $CeNiSnH_{1.8}$ respectively.[13] This comparison suggests that the electrical resistivity of $CeNiGaH_{1.1(1)}$ is strongly affected by the structural disorder (Ni-Ga distribution and partial occupancy of the H site).

Interesting features can be observed on the curve ρ(T) = f(log T) relative to $CeNiGaH_{1.1(1)}$ (Fig. 4): (i) below 210 K, ρ(T) increases with decreasing temperature up to a broad maximum appearing around 98 K; (ii) below this maximum, ρ decreases and a minimum occurs near 20 K; (iii) finally, below this minimum there is a rise of ρ(T) down to 1.8 K. In the two temperature ranges 120 K - 180 K and 3 K – 10 K (inset of Fig. 4), the law ρ(T) = -A log T (A = constant) is observed. Such behavior is expected for Kondo-type interactions in the presence of crystal field effects.[14] The high-temperature logarithmic region represents the Kondo effect in the excited doublet, whereas the low-temperature region is relative to the Kondo effect from the crystal field ground state. The maximum on the curve ρ(T) = f(log T) occurring between these two temperature ranges, is related to the crystal field splitting. We note that the temperature (98 K) of this maximum is close to that (100 K) where the curve χ_m^{-1} = f(T) deviates from the Curie-Weiss law.[5] It is interesting to note that below 3 K, the resistivity deviates negatively from the law ρ(T) = -A log T, suggesting the influence of magnetic correlations.

The curve S = f(T) of the thermoelectric power plotted as a function of the temperature of the two crystallographic forms of CeNiGa and its hydride $CeNiGaH_{1.1(1)}$ are shown for the 4.2 – 300 K temperature range in Fig. 5. The two curves S = f(T) relative to CeNiGa LTF and HTF are in agreement with their electrical properties. Below 300 K, the positive sign of S for the former implies that the dominant carriers are holes. For this ternary gallide, S decreases linearly from 28(1) to 8(1) μV/K with the temperature between 300 and 90 K, takes a constant value in the temperature range 90 – 30 K and goes towards zero with decreasing temperature. This is the typical behavior of the valence fluctuating cerium compounds with a very high Kondo temperature as $CeNi_2Si_2$ [15], $CeNi_3$ [16] or $Ce(Pd_{0.85}Rh_{0.15})_3$.[17] The curve S = f(T) of CeNiGa HTF shows a clearly different behavior. It is mainly characterized by the existence of a positive maximum of about 10.5(5) μV/K near 75 K and a shoulder around 20 – 30 K. This curve resembles that observed for $CePd_3$ which is well known as a canonical intermediate valence compound.[18, 19] The insertion of hydrogen into the CeNiGa lattice drastically changes the temperature dependence of its thermoelectric power (Fig. 5). At room temperature, S of $CeNiGaH_{1.1(1)}$ is close to zero. Also, the position of the maximum appearing on the curve shifts towards low temperatures (~ 40 K) and the absolute value of the maximum is reduced by a factor of almost two in comparison to the curve relative to CeNiGa HTF. Similar behavior was observed for the solid solution $Ce(Pd_{1-x}Ag_x)_3$ where the replacement of Pd by Ag induces a valence transition for cerium from the intermediate valence state ($CePd_3$) to a purely trivalent state ($Ce(Pd_{0.87}Ag_{0.13})_3$.[17] The evolution of the curves S = f(T) in the sequence CeNiGa LTF → CeNiGa HTF → $CeNiGaH_{1.1(1)}$ is in agreement with the evolution of the

valence of cerium (intermediate valence state → trivalent state) deduced by magnetization measurements.[5]

C. Specific heat

The specific heat (C_p) of $CeNiGaH_{1.1(1)}$ has been measured at zero magnetic field between 2 K and 300 K (Fig. 6). No λ-transition characteristic of magnetic order is observed anywhere along the whole temperature range. The increase of C_p with temperature is mainly due to the phonon contribution. In addition, we should have electronic and crystal field contributions. In the hexagonal system, as for this hydride, the sixfold degenerated 4-f state of Ce^{3+} ions (J = 5/2) splits into three doublets, with the excited states separated from the ground state by energy gaps Δ_1 and Δ_2. In order to determine the splitting of the ground multiplet, the experimental $C_p(T)$ was fitted to the addition of three contributions:

$$C_p(T) = C_{el}(T) + C_{ph}(T) + C_{CEF}(T)$$

(i) the electronic part $C_{el}(T) = \gamma_{HT}\, T$ was taken as linearly temperature dependent; (ii) in absence of non f-electron reference compound isomorphous to $CeNiGaH_{1.1(1)}$, the phonon contribution $C_{ph}(T)$ was assumed to follow a Debye model but, due to the important different weight of the constituents, we consider two different phonon spectra, each associated to a Debye temperature θ_D: $C_{ph}(T) = n_1\, C_{ph}(\theta_{D1}) + n_2\, C_{ph}(\theta_{D2})$ where $n_1 = 3$ corresponds to the number of atoms in the mol of CeNiGa and $n_2 = 1.1$ to that of H-atoms by mol of CeNiGa and $C_{ph}(\theta_D) = C_{ph}(T) = 9\, R\, (T/\theta_D)^3\, ?_0^{\theta_D/T} [(x^4\, e^x\, dx) / (e^x - 1)^2]$; (iii) C_{CEF} is due to the crystal electric field effect $C_{CEF} = \dfrac{1}{K_B T^2} \dfrac{\Delta_1^2\, e^{-\Delta_1/K_B T} + \Delta_2^2\, e^{-\Delta_2/K_B T} + [\Delta_1 + \Delta_2]^2\, e^{-(\Delta_1+\Delta_2)/K_B T}}{\left[1 + e^{-\Delta_1/K_B T} + e^{-\Delta_2/K_B T}\right]^2}$. The best fitting between 25 K and 300 K (see the continuous line in Fig. 6) is obtained for $\gamma_{HT} = 18$ mJ/mol K^2 as the Sommerfeld coefficient, $\theta_{D1} = 279$ K and $\theta_{D2} = 1223$ K as Debye temperatures and the contribution from the crystal electric field excitation to the specific heat (Fig. 6) gives the energy splitting $\Delta_1 = 100$ K and $\Delta_2 = 159$ K from the ground state, respectively. Although neutron diffraction experiments are necessary to check this CEF energy splitting scheme, we should stress that the fitting is very good (the fitted curve is over experimental points all along the entire temperature range) and the obtained values of the Debye temperatures and CEF splitting are quite reasonable. In fact, we note that according to Cornut and Coqblin,[14] the high temperature maximum of the electrical resistivity (Fig. 4) takes place at a temperature slightly lower than that of the overall CEF splitting. In $CeNiGaH_{1.1(1)}$, the calculated value of $\Delta_1 = 100$ K is in rather good agreement with the temperature of the maximum (98 K) of $\rho = f(T)$ curve.

At low temperatures (see inset of Fig. 6), a very small and broad anomaly is observed near 4 K. This contains a very small amount of magnetic entropy of $S_{mag}/R = 0.10$ per Ce atom (corresponding to only 14 % of the value ln 2 expected for magnetic ordering of a crystalline-electric-field ground state doublet). This result excludes the occurrence of a long-range spatial magnetic ordering and indicates that the magnetic correlations are weaker. When we plot the specific heat in a C_p/T versus T^2 format (see figure 7), a linear region is observed above 13 K; therefore, we can obtain the electronic coefficient γ_{LT} by fitting the data to the formula $C_p/T = \gamma_{LT} + \beta_{LT} T^2$. The obtained values for the temperature range 13 K<T<23 K were $\gamma_{LT} = 55$ mJ/mol K^2 and $\beta_{LT} = 0.412$ mJ/mol K^4. Considering this value of γ_{LT}, we could define our hydride as a non heavy fermion system; however, it is important to note that below 10 K, the C_p/T curve departs markedly from the linearity, reaching a large value of 352 mJ/mol K^2 at 2 K. Similar behavior was observed in many compounds considered as

nonmagnetic atom disorder spin glasses. [20] For instance, the random distribution of boron in $CePd_3B_{0.3}$ introduces a varying electronic environment around the Ce-atoms and causes an increase in C_p/T at low temperature.

To understand the origin of the very small and broad anomaly in the specific heat, we have analysed the existing literature. In particular, a similar broad maximum in C_p was found in Ce_xSi_{100-x} amorphous alloys around 4 K.[21] In this case C_p/T also increases at low temperatures reaching large values (for example, 450 mJ/mol K^2 for x = 66 sample). In addition, the magnetization increases by decreasing the temperature, without there being any signature of magnetic transition. This behavior was interpreted as being due to the atomic randomness which suppress the coherently ordered state such as degenerate Fermi liquid and the magnetic ordered state observed in the crystalline counterparts. Further ZC-ZFC susceptibility measurements down to 1.8 K in the same Ce_xSi_{100-x} amorphous family reveal the existence of spin glass transition around 2.5 K. [22] From this point of view, we should remember that, according to Mydosh [12], a broad transition at temperatures higher than the freezing one could appear in the heat capacity of spin-glasses.

The effects of the magnetic field on the C_p values in fields up to 9 T are shown in figure 8. We found that the magnetic field has a strong influence on the C_p values at low temperatures, its effects diminishing as the temperature increases, and being negligible above 25 K. The behavior is the following: below 25 K, C_p increases with the field, whereas at the lowest temperature C_p decreases, so the very broad maximum appearing on the curve of C_p at zero field moves to higher temperature with an increasing magnetic field. That means that the magnetic field transfers entropy from the lowest temperature region to the higher ones. This evolution of entropy with magnetic field is typical not only in ferromagnetic systems, but also in spin glass materials.[12] Indeed, in the previously mentioned Ce_xSi_{100-x} amorphous compounds, the C_p peak position was found to shift to higher temperatures with the increasing magnetic field. [22] Other compounds with similar behaviour are $Ce_{0.1}Th_{0.9}Cu_2Si_2$ [23], and Ce_2CuGe_3 [8] and in both cases spin glass (or cluster glass) behavior was suggested as its origin. In particular, the last compound belongs to the family R_2TX_3 (R = U, Ce; T = transition metal and X = Ge, Si) in which the statistical distribution of T and X atoms at crystallographically equivalent lattice sites usually gives rises to random exchange interactions between R ions which favour the apparition of spin glasses behavior [7] In our case, it is worth mentioning that in addition to the disorder between Ni and Ga atoms, there is a random distribution of the hydrogen position inside the lattice, which certainly increases the randomness of: (i) the exchange interactions and (ii) the local magnetic anisotropy, thereby provoking the occurrence of the spin glass behavior at low temperatures.

Therefore, in view of the different models which could account for our specific heat and its evolution with magnetic field, and discarding the existence of a long range magnetic order, the most likely explanation is the following: magnetic correlations or even short range magnetic order emerge by decreasing the temperature below 4 K as a previous state of the spin glass freezing which occurs below T_f <1.8 K. A similar scenario is that paramagnetic random magnetic moments correlate to form magnetic clusters below 4 K and those magnetic clusters are frozen in a cluster glass phase below T_f, losing their dynamical aspect. In both cases, the existence of short range magnetic order prior to the freezing process could explain both the occurrence of small irreversibility in the susceptibility below 4 K and the small anomaly in C_p.

Our last comment is about the γ_{LT} coefficient which, although not large enough to consider $CeNiGaH_{1.1}$ as a heavy fermion, is one order of magnitude larger that the expected in the free electron model. In this sense, Gschneidner et al.[20] indicate that large C_p/T values may mislead one to classify a spin glass within a heavy fermion system. In fact, they pointed out

that the possible mechanism that will enhance the C_p/T values are : (i) low lying crystal fields levels, (ii) a spin glass phase, and (iii) magnetic order at low temperature. Because point (iii) is already discarded, we proceeded to investigate the influence of the crystal field. We subtracted from the total heat capacity the CEF contribution previously determined and then used these data to recalculate γ_{LT}. Because Δ_1= 100 K is relatively larger, the CEF subtraction primarily reduces the slope of the specific heat curve and consequently enhances the γ value in a C_p/T versus T^2 representation (see figure 7). Therefore the CEF corrected value γ_{LT} = 61 mJ/mol K^2 is even higher than the uncorrected one (55 mJ/mol K^2) as was also determined in $CePb_3$ [24]. This observation discards point (i) as well, and thus supports the existence of a spin glass transition as the origin of the large C_p/T values at low temperatures.

D. Magnetoresistivity

Fig. 9 shows at different temperatures the magnetoresistivity (MR) defined by $(\rho(\mu_0 H) - \rho(0\ T)) / \rho(0\ T)$ as a function of applied magnetic fields for $CeNiGaH_{1.1(1)}$. Above 25 K, MR is small, always positive and increases with decreasing temperatures; for $\mu_0 H$ = 9 T, MR is equal to +0.03% and 0.04% at T = 50 K and 25 K respectively. This behavior indicates that the Kondo effect is so weak in this temperature range that MR is dominated by the positive contribution arising from the influence of $\mu_0 H$ on the conduction electrons. At T = 10 K, MR is positive at low fields, passes through a maximum near $\mu_0 H$ = 3 T and changes in sign around $\mu_0 H$ = 5 T. Below 10 K, MR is always negative and its magnitude increases with decreasing temperatures; MR measured at $\mu_0 H$ = 9 T is about –0.27%, -0.50% and –0.73% for T = 5 K, 3 K and 2 K respectively. In this temperature range T<10 K, the negative MR is due to the freezing out of spin-flip scattering in a Kondo compound by the magnetic applied field. We have fitted the data (Fig. 9b) with an $-a\ (\mu_0 H)^2$ law usually appearing in Kondo systems. At T = 5 K, a quadratic field dependence is observed at least up to $\mu_0 H$ = 9 T; the constant value a is equal to 3.39 10^{-3} $\%T^{-2}$. Below T = 5 K, the range over which the $-a\ (\mu_0 H)^2$ dependence holds decreases as the temperature is lowered; for instance at 3 K and 2 K, this law is respectively followed for $(\mu_0 H)$<5.9 T and $(\mu_0 H)$<3.2 T. These deviations indicate for T<5 K the influence of magnetic correlations. This study confirms the presence of Kondo fluctuations in $CeNiGaH_{1.1(1)}$ which influences its magnetoresistivity below T<10 K.

IV. Conclusion

The hydride $CeNiGaH_{1.1}$ crystallizes in the hexagonal AlB_2-type structure with a random distribution of nickel and gallium atoms on the B site. Moreover, the partial occupancy of the crystallographic site devoted to the H-atoms also induces structural disorder around the Ce-atoms. The magnetization, electrical resistivity, specific heat and magnetoresistivity measurements presented here confirm that this hydride does not show detectable long-range magnetic ordering down to 1.8 K. But this study reveals some characteristic features of nonmagnetic atom-disorder spin glasses : (i) a small irreversibility effect appears below 4 K in the thermal dependence of its magnetization; (ii) its electrical resistivity deviates negatively below 3 K from the law $\rho(T) = -A \log T$ suggesting the presence of magnetic correlations; (iii) near 4 K, a broad maximum is detected on the curve $C_p = f(T)$; this maximum moves to a higher temperature with an increasing magnetic field; (iv) finally, at low temperatures, its magnetoresistivity results from a competition between the Kondo effect and the magnetic correlations. Heat capacity up to room temperature allows us to determine the Schottky type anomaly associated to the ground multiplet of Ce^{3+} ions (J = 5/2). These results confirm than the negative pressure produced by hydrogen insertion in CeNiGa induces a change from intermediate valence to a trivalent state in the Ce ions and gives rise to the appearance of spin glass behavior at low temperatures.

Acknowledgements

This work was partially supported by EGIDE (France) through the Picasso program and CICYT though the Acciones Integradas program (HF2001-32) and MAT 2002-04178-C04-04.

.

References

[1] S. S. Saxena, P. Agarwal, K. Ahilan, F. M. Grosche, R. K. W. Haselwimmer, M. J. Steiner, E. Pugh, I. R. Walker, S. R. Julian, P. Monthoux, G. G. Lonzarich, A. Huxley, I. Sheiklin, D. Braithwaite and J. Flouquet, Nature **406**, 587 (2000).
[2] C. Pfleiderer, S. R. Julian and G. G. Lonzarich, Nature **414**, 427 (2001).
[3] I. Mirebeau, I. N. Goncharenko, P. Cadavez-Peres, S. T. Branwell, M. J. P. Gingras and J. S. Gardner, Nature **420**, 54 (2002).
[4] S. Doniach, Physica B **91**, 231 (1977).
[5] B. Chevalier, J.-L. Bobet, E. Gaudin, M. Pasturel and J. Etourneau, J. Solid State Chem. **168**, 28 (2002).
[6] A. de Visser, F. E. Kayzel, A. A. Menovsky, J. J. M. Franse, J. Van den Berg and G. J. Nieuwenhuys, Phys. Rev. B **34**, 8168 (1986).
[7] D. Huo, J. Sakurai, O. Maruyama, T. Kuwai, Y. Isikawa and Q. Lu, Phys. Rev. B, **64**, 224405 (2001).
[8] Cheng Tien, Chang Hsing Feng, Ching Shui Wur and Jenq Jong Lu, Phys. Rev. B **61**, 12151 (2000).
[9] P. Dordor, E. Marquestaut and G. Villeneuve, Rev. Phys. Appl. **15**, 1607 (1980).
[10] B. Chevalier, J. –L. Bobet, M. Pasturel, E. Bauer, F. Weill, R. Decourt and J. Etourneau, Chem. Mater. **15**, 2181 (2003).
[11] J. –L. Bobet, B. Chevalier, B. Darriet, M. Nakhl, F. Weill, J. Etourneau, J. Alloys Comp. **317-318**, 67 (2001).
[12] J. A. Mydosh, Spin Glass: An Experimental Introduction, Taylor § Francis, London, (1993).
[13] B. Chevalier, M. Pasturel, J. –L. Bobet, J. Etourneau, O. Isnard, J. Sanchez Marcos, J. Rodriguez Fernandez, J. Magn. Magn. Mat., **272-276**, 576 (2004).
[14] B. Cornut and B. Coqblin, Phys. Rev. B, **5**, 4541 (1972).
[15] D. Huo, J. Sakurai, O. Maruyama, T. Kuwai, Y. Isikawa, J. Magn. Magn. Mat. **226-230**, 202 (2001).
[16] U. Gottwick, K. Gloos, S. Horn, F. Steglich and N. Grewe, J. Magn. Magn. Mat. **47-48**, 536 (1985).
[17] H. Sthioul, D. Jaccard and J. Sierro, in Valence Instabilities, P. Wachter and H. Boppart (Eds), North-Holland, Amsterdam, (1982) p. 443.
[18] D. Jaccard and J. Sierro, in Valence Instabilities, P. Wachter and H. Boppart (Eds), North-Holland, Amsterdam, (1982) p. 409.
[19] M. Houshiar, D. T. Adroja, B. D. Rainford, Physica B **223-224**, 268 (1996).
[20] K. A. Gschneidner, Jr., J. Tang, S. K. Dhar and A. Goldman, Physica B **163**, 507 (1990).
[21] T. Hihara, K. Sumiyama, H. Yamauchi, Y. Homma, T. Suzuki and K. Suzuki, J. Phys.: Condens. Matter **5**, 8425 (1993).
[22] T. Biwa, M. Yui, T. Takeuchi and U. Mizutani, Mat. Trans., **42**, 939 (2001).
[23] J. S.Kim, C. S. Jee, W. W. Kim, B. Andraka, P. Kumar and G. R. Stewart, Phys. Rev. B **44**, 7473 (1991).

[24] N. Pillmayr, G. Hilscher, W. Perthold, J. Sakurai and M. Horie, J. Magn. Magn. Mat. **90-91,** 414 (1990).

Figure captions

Fig.1 Electron diffraction patterns of $CeNiGaH_{1.1(1)}$ (a) and $CeNiSnH_{1.8(2)}$ (b) along the [0 –1 0] direction.

Fig. 2 Temperature dependence at $\mu_0 H$ = 25 Oe of the zero-field-cooled (ZFC) and field-cooled (FC) magnetic susceptibility of hydride $CeNiGaH_{1.1(1)}$.

Fig. 3 Field dependence at 2 K of the magnetization of $CeNiGaH_{1.1(1)}$ measured with an increasing and decreasing applied magnetic field. Inset for the low magnetic field range.

Fig. 4 Electrical resistivity as a function of log T for $CeNiGaH_{1.1(1)}$. The inset shows the temperature dependence for $T \leq 10$ K; the solid line represents the fit –A log T.

Fig. 5 Temperature dependence of the thermoelectric power for the ternary gallide CeNiGa LTF and HTF and its hydride $CeNiGaH_{1.1(1)}$.

Fig. 6 Temperature dependence of the specific heat of $CeNiGaH_{1.1(1)}$ in a zero applied magnetic field. Experimental data (full points), fitting curve (full line) and contribution from the crystal electric field excitation (open circles). The inset shows the low temperature part for $T \leq 10$ K.

Fig. 7 The C_p/T versus T^2 of $CeNiGaH_{1.1(1)}$ in H = 0. Experimental data are plotted as filled squares (■), whereas the empty squares (□) have been obtained after subtracting the crystal field contribution. The lines represent fits to the data showing the γ_{LT} value, see text.

Fig. 8 Temperature dependence of the specific heat for $CeNiGaH_{1.1(1)}$ in different applied magnetic fields.

Fig. 9 Field dependence of magnetoresistivity for $CeNiGaH_{1.1(1)}$ in the temperature range 5 K $\leq T \leq$ 50 K (a) and 2 K $\leq T \leq$ 10 K (b). The dotted lines are relative to the fit with $-a(\mu_0 H)^2$ expression.

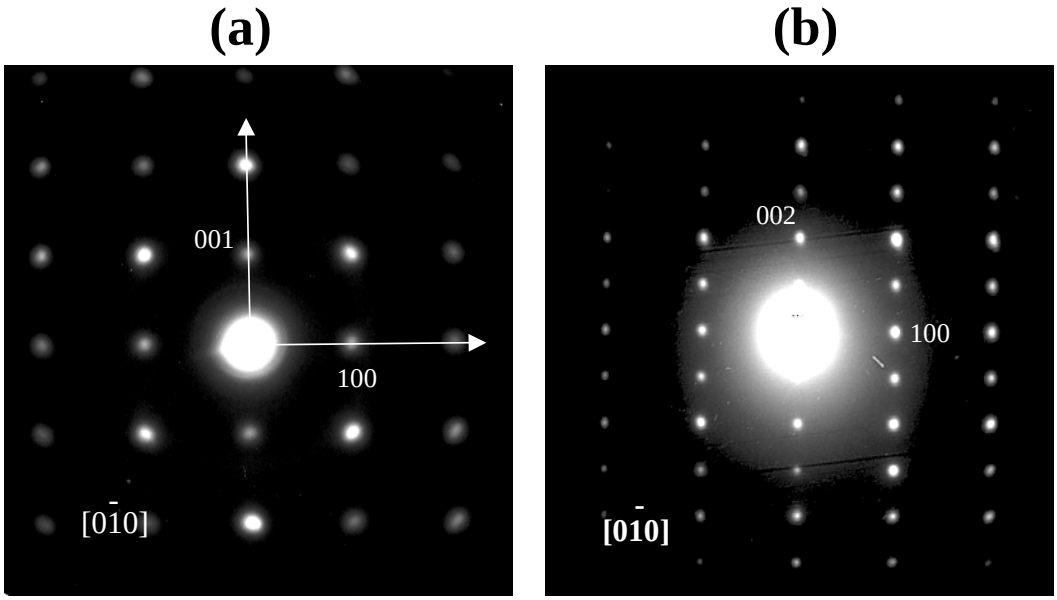

Fig.1 Electron diffraction patterns of $CeNiGaH_{1.1(1)}$ (a) and $CeNiSnH_{1.8(2)}$ (b) along the [0 –1 0] direction.

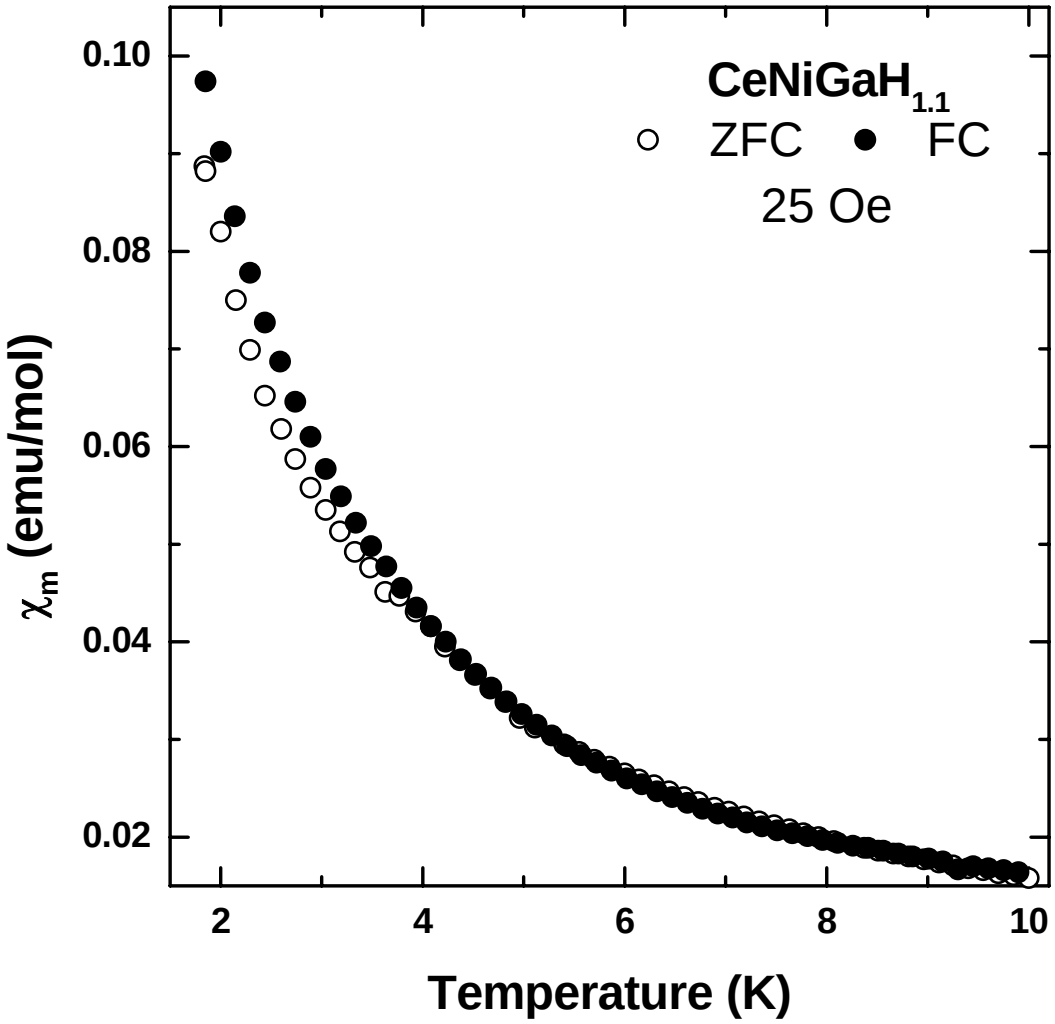

Fig. 2 Temperature dependence at $\mu_0 H$ = 25 Oe of the zero-field-cooled (ZFC) and field-cooled (FC) magnetic susceptibility of hydride $CeNiGaH_{1.1(1)}$.

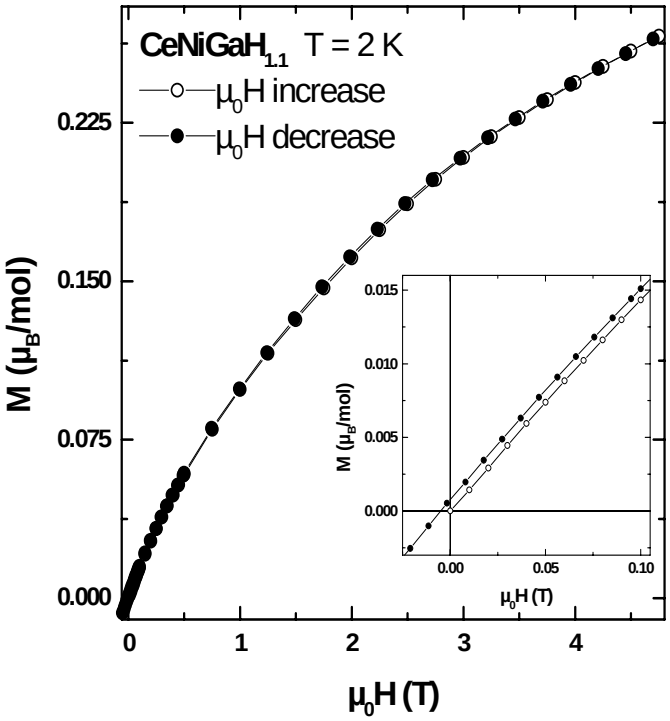

Fig. 3 Field dependence at 2 K of the magnetization of $CeNiGaH_{1.1(1)}$ measured with an increasing and decreasing applied magnetic field. Inset for the low magnetic field range.

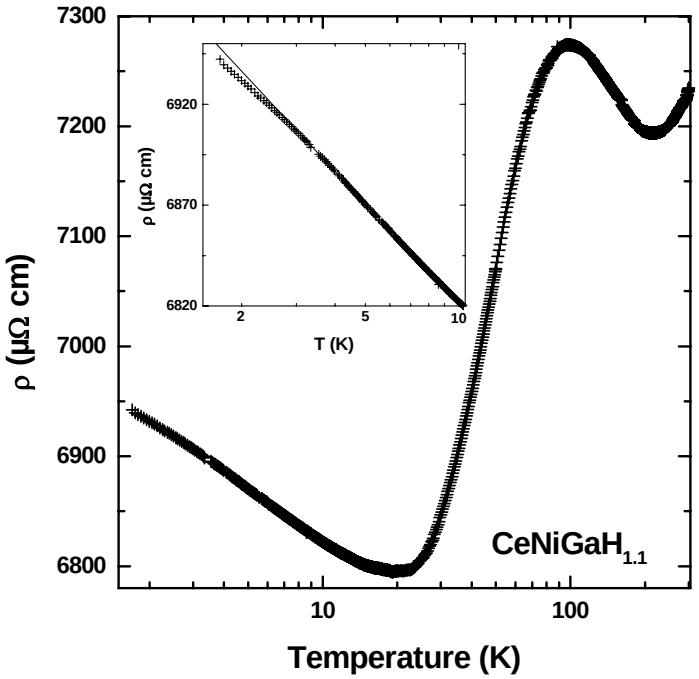

Fig. 4 Electrical resistivity as a function of log T for $CeNiGaH_{1.1(1)}$. The inset shows the temperature dependence for $T \leq 10$ K; the solid line represents the fit $\rho = -A \log T$.

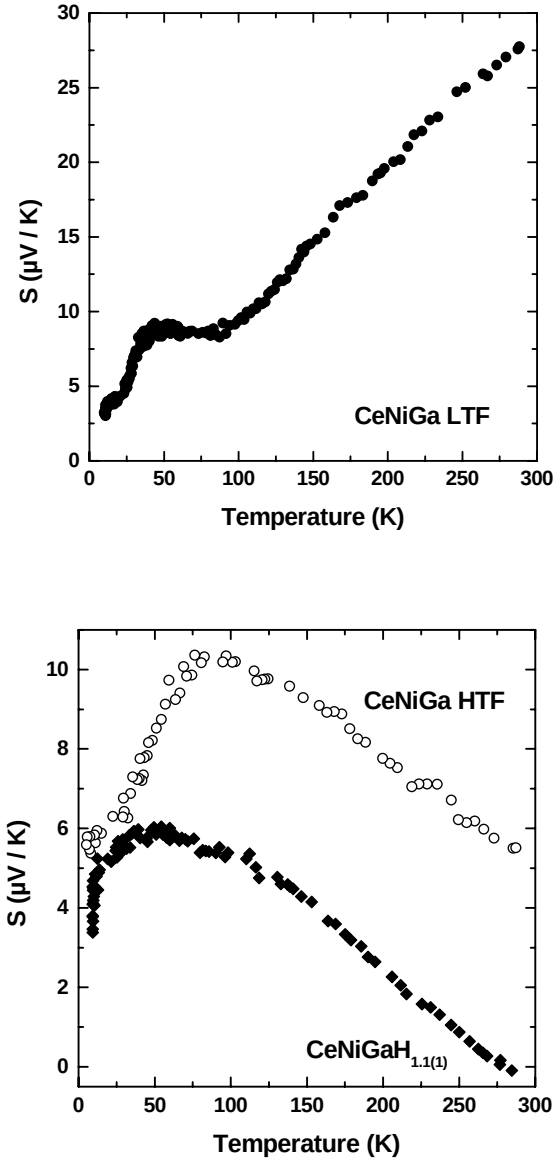

Fig. 5 Temperature dependence of the thermoelectric power for the ternary gallide CeNiGa LTF and HTF and its hydride $CeNiGaH_{1.1(1)}$.

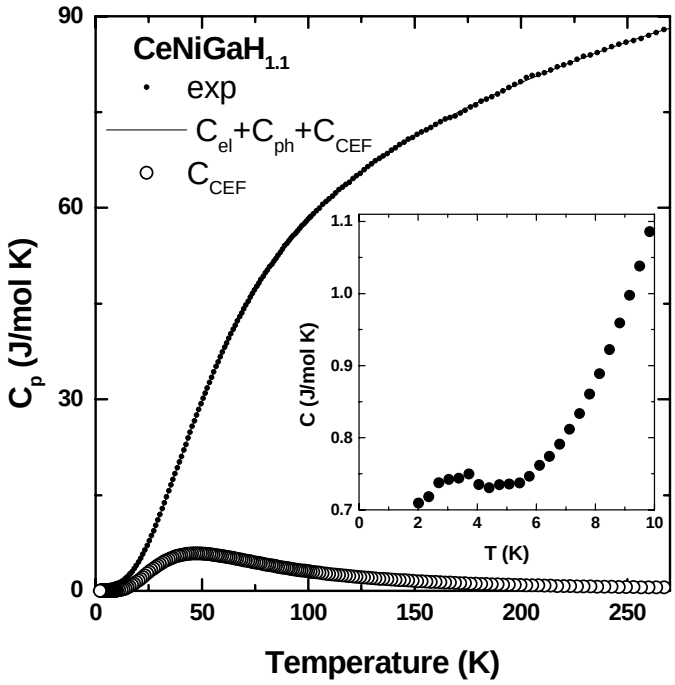

Fig. 6 Temperature dependence of the specific heat of $CeNiGaH_{1.1(1)}$ in a zero applied magnetic field. Experimental data (full points), fitting curve (full line) and contribution from the crystal electric field excitation (open circles). The inset shows the low temperature part for $T \leq 10$ K.

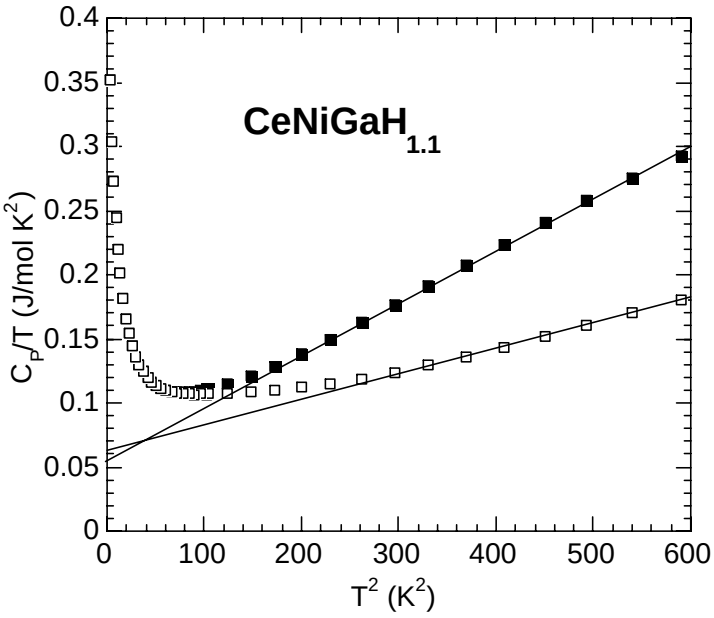

Fig. 7 The C_p/T versus T^2 of $CeNiGaH_{1.1(1)}$ in H = 0. Experimental data are plotted as filled squares (■), whereas the empty squares (□) have been obtained after subtracting the crystal field contribution. The lines represent fits to the data showing the γ_{LT} value, see text.

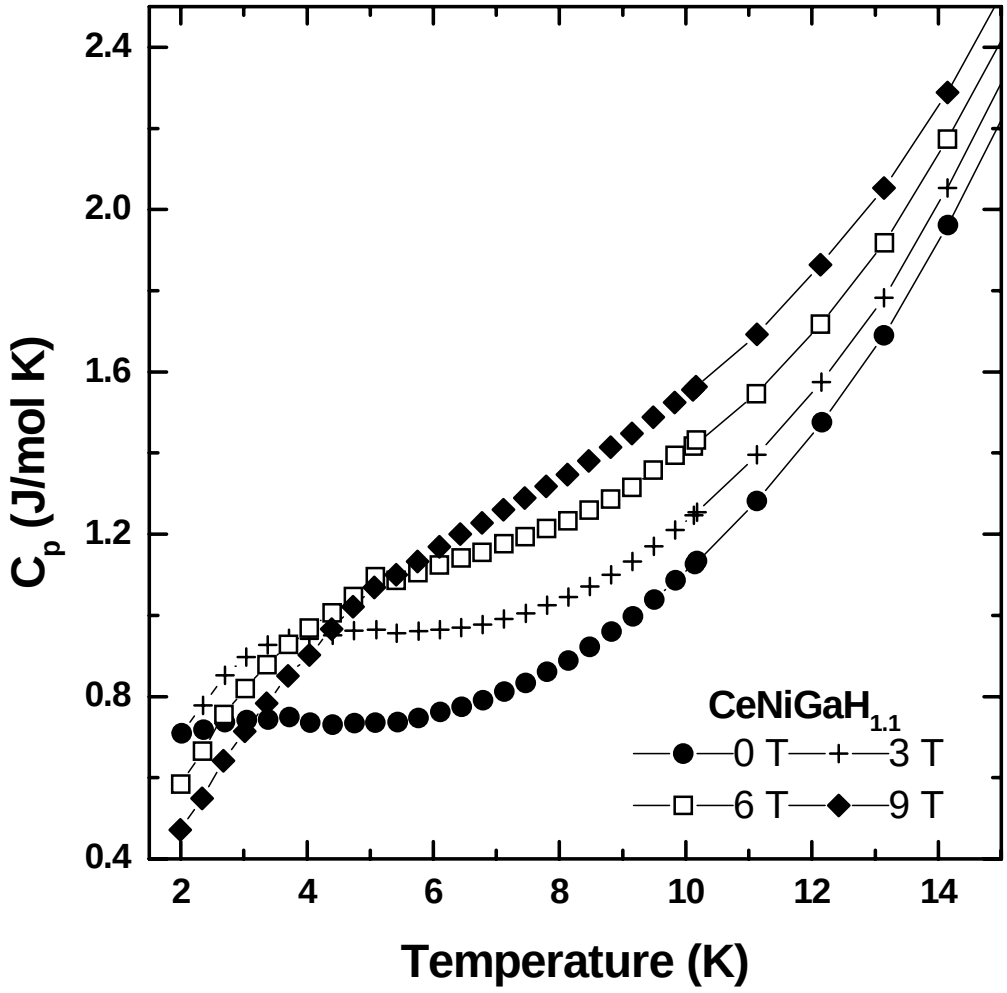

Fig.8 Temperature dependence of the specific heat for $CeNiGaH_{1.1(1)}$ in different applied magnetic fields.

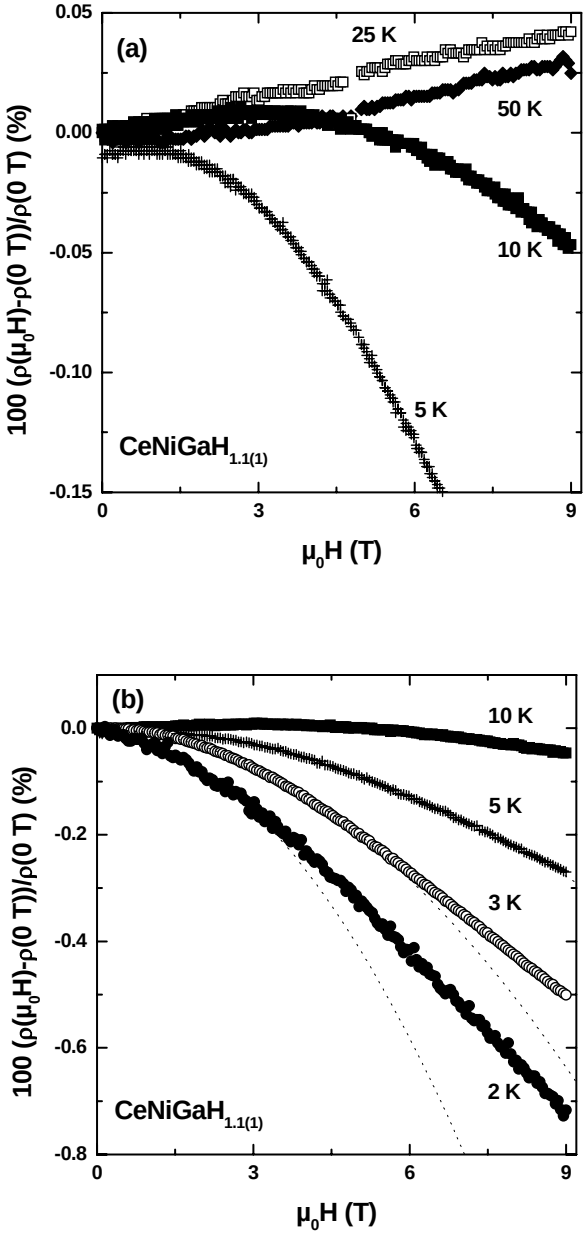

Fig.9 Field dependence of magnetoresistivity for $CeNiGaH_{1.1(1)}$ in the temperature range 5 K ≤ T ≤ 50 K (a) and 2 K ≤ T ≤ 10 K (b). The dotted lines are relative to the fit with –a $(\mu_0 H)^2$ expression.